HORMONAL REGULATION OF GAP JUNCTION DIFFERENTIATION

ROBERT S. DECKER

From the Department of Cell Biology, University of Texas Health Science Center, Southwestern Medical School, Dallas, Texas 75235

ABSTRACT

Thin-section, tracer, and freeze-cleave experiments on hypophysectomized *Rana pipiens* larvae reveal that gap junctions form between differentiating ependymoglial cells in response to thyroid hormone. These junctions assemble in large particle-free areas of the plasma membrane known as formation plaques. Between 20 and 40 h after hormone application, formation plaque area increases approximately 26-fold while gap junction area rises about 20-fold. The differentiation of these junctions requires the synthesis of new protein and probably RNA as well. On the basis of inhibitor experiments, it can be reported that formation plaques develop at about 16–20 h after hormone treatment and stages in the construction of gap junctions appear 4–8 h later. These studies suggest that gap junction subunits are synthesized and inserted into formation plaque membrane during the differentiation of the anuran ependymoglial cells.

Recent observations on the construction of gap junctions in vitro (18) as well as in vivo (1, 3, 6, 35, 36, 48) portray junctional precursors assembling in an orderly fashion. Common features among developing gap junctions include the: (*a*) appearance of formation plaques (18); (*b*) clustering and/or aggregation of large precursor particles accompanying a reduction of the extracellular space; (*c*) polygonal packing of particles into recognizable junctions; and (*d*) enlargement of junctions through the recruitment of nearby granules and/or fusion of smaller aggregates (1, 3, 6, 18, 36). Although minor variations on this theme may exist (3), the similarities are truly remarkable. Moreover, the developing gap junction provides an ideal model system to assess some of the macromolecular requirements for regional plasma membrane differentiation.

While a morphological picture of gap junction assembly is slowly emerging, macromolecular events concerned with the control of junctional differentiation remain to be elucidated. In one instance, the coordinate appearance of gap junctions and electrotonic coupling between reaggregating Novikoff hepatoma cells (18) appears insensitive to drugs like cycloheximide (9) which inhibit protein synthesis. In another, cycloheximide prevents cell-cell interaction between cultured myoblasts (47) and, therefore, may preclude the development of gap junctions and low-resistance coupling (33) between these cells. Events accompanying myoblast fusion (47) imply that the production of new membrane proteins is essential in the development of multinucleate myotubes. The synthesis and insertion of gap proteins into the myoblast plasma membrane are thought to be crucial in the coordination of myogenic cell fusion (33).

The present experiments, employing hypophysectomized *Rana pipiens* larvae, reveal that the synchronous differentiation of ependymoglial cells requires thyroid hormones. One feature of glial

differentiation encompasses the formation of gap junctions between adjacent cells. The mode of junctional assembly resembles that depicted in reaggregation of Novikoff hepatoma cells (18); however, new protein synthesis is an absolute requirement for junctional formation during thyroxine-mediated glial differentiation.

MATERIALS AND METHODS

Animal Care

All tadpoles were reared and cared for as described previously (6). When the embryos reached embryonic stage 17 (42) they were chosen for hypophysectomy. At this point in development, a wedge of pigmented ectoderm, including a portion of the hypophyseal pit, was surgically removed with glass needles and hair loops. The embryos were left in the operating medium (2× Holtfreter's solution) for 30 min to heal and then returned to standard Holtfreter's solution until they began to feed. Successfully hypophysectomized larvae revealed an unpigmented or "silvery" appearance, and did not progress beyond Taylor and Kollros (45) stages VI or VII. Only those larvae which exhibited a steady rate of growth were employed in this investigation.

Hormone Administration

Stage VII tadpoles with hind limb length to body length ratios of less than 0.05 were given a single injection of 1.0 μg/g body weight of DL-thyroxine (Sigma Chemical Company, St. Louis, Mo.) intraperitoneally. Control larvae received 200 μN NaOH (the vehicle in which the hormone is suspended) instead of DL-thyroxine. The larvae were carefully staged (45) and preserved for light and electron microscopy at 4-h intervals through the first 48 h and, thereafter, at daily intervals.

Morphology

The medullary region of selected tadpoles was preserved by vascular perfusion as reported earlier (6). The primary fixative consisted of 1.67% glutaraldehyde, 1.33% paraformaldehyde, and 0.5% acrolein buffered at pH 7.4 with 0.1 M sodium cacodylate. Occasionally, 2.5% dimethylsulfoxide was added to facilitate penetration of the fixative. In some experiments, $CaCl_2$ (25 mM) was replaced by 1% potassium pyroantimonate in the fixative to enhance junctional staining; in others, heavy metal tracers, such as colloidal lanthanum (3%), potassium pyroantimonate (5%), or ruthenium red (500 ppm), were administered in the fixative (6). Larvae were perfused for 15–20 min and, after a 2–3-h delay, medullary tissue was diced and fixation was continued for another 8 h. Tissues were washed overnight in 0.1 M cacodylate buffer (pH 7.4) with 7% sucrose and then postfixed in 1% OsO_4 plus 5% sucrose for 1–2 h. Subsequently, tissue slices were rinsed for 1–2 h in 0.5% uranyl acetate (pH 5.5), rapidly dehydrated in ethanol and propylene oxide, and embedded in Epon 812.

Silver or gray thin sections were obtained on a Porter-Blum MT-2 ultramicrotome, (DuPont Instruments, Sorvall Operations, Newtown, Conn.) equipped with a DuPont diamond knife (E. J. DuPont de Nemours, Inc., Wilmington, Del.). They were picked up on carbon-stabilized and Formvar-coated 200-mesh grids, stained in 5% aqueous uranyl acetate followed by alkaline lead, and viewed in a Siemens Ia or Philips 200 electron microscope.

Freeze Fracturing

Small pieces of briefly (15 min) fixed medulla were immersed in 0.1 M cacodylate-buffered (pH 7.4) 20% glycerol. After the tissues had been treated for a minimum of 4 h at 4°C, they were mounted on cardboard disks and rapidly frozen in liquid Freon 22 cooled in liquid nitrogen. The samples were then fractured at −115°C and shadowed with platinum and carbon in a Balzers' apparatus (BA360M, Balzers High Vacuum Corp., Santa Ana, Calif.). Replicas were cleaned in sodium hypochlorite and viewed in a Siemens Ia or Philips 200 electron microscope.

The surface area of A-face membrane, formation plaques, and gap junctions derived from replicas was determined with a compensating polar planimeter (model no. 620015, Keuffel and Esser Co., Morristown, N. J.). Only micrographs which revealed formation plaques and/or gap junctions on the A face of the plasma membrane were selected and measured from each experiment. B-face profiles were not utilized because of the uncertainty of formation plaque boundaries on this portion of the cell membrane. The area of the A-face plasma membrane which represents either formation plaques or gap junctions is expressed as formation plaque or gap junction area (square micrometers) per 100 μm^2 of A-face membrane. From each experimental animal, at least 10 plaque regions were randomly selected from available micrographs and measured.

Incorporation of [^{3}H]Uridine

After the injection of a single dose of DL-thyroxine, 5.0 μCi/g body weight of [5-^{3}H]uridine (sp act 20.0 mCi/mmole, ICN Isotope and Nuclear Division, Irvine, Calif.) were administered intraperitoneally through the tail musculature to prevent leakage of the isotope. The nucleoside was injected 1 h before larval sacrifice at 0, 4, 8, 12, 16, 20, 24, 36, or 48 h after hormone treatment. The ependymal epithelia of five tadpoles were carefully removed and homogenized in 1 ml of 50 mM Tris (pH 7.4), 5 mM $MgCl_2$, 25 mM KCl, and 0.32 M ribonuclease-free sucrose. One aliquot of the homogenate was retained to measure the activity of the acid-soluble nucleotide pool; the remaining portion was centrifuged at 800 *g* for 10 min. These samples were treated with 1 vol of ice-cold 0.6 N perchloric acid (PCA). The sediments

from the whole homogenate and the 800-*g* fraction were washed twice in cold 0.2 N PCA, and the supernates were retained to measure the specific activity of the acid-soluble pool.

A sample of the PCA-soluble extract was evaporated in a vacuum desiccator and the residue was dissolved in 50 μl of water. This fraction was applied to a column of Dowex 50 W X4 (50–100 mesh) which had a bed volume of 1.0 ml and a void volume of 50 μl. A fraction was obtained that possessed 95–97% of the uridine derivatives and radioactivity. This fraction was used to determine the specific activity of the nucleotide pool.

The acid-insoluble extracts (RNA fractions) were suspended in 0.3 N KOH and incubated for 18 h at 37°C. The hydrolysates were cooled, acidified with 0.7 N PCA, and centrifuged. The DNA and protein precipitates were subjected to two further washings in 0.2 N PCA, and the supernates were combined and the optical density was determined at 260 nm in a Beckman DU spectrophotometer (Beckman Instruments, Inc., Fullerton, Calif.). An extinction coefficient of 34.2 cm^2/mg was adopted to calculate RNA concentration (10).

Samples of acid-soluble fractions or RNA extracts were neutralized with 1 N KOH to precipitate maximum amounts of perchlorate, and aliquots of the supernates were mixed with 5 ml of scintillation fluid (2 parts of toluene containing 0.4% 2,5-diphenyloxazole [PPO] and 0.1% 1,4 bis-2-(5 phenyloxozolyl)-benzene [POPOP] and 1 part Triton X-100). Radioactivity was monitored in a Beckman LS-250 liquid scintillation counter. Alterations in the specific activity of the acid-soluble pool were expressed as cpm/OD 260 nm, whereas the incorporation of tritiated uridine into acid-precipitable material (RNA fraction) was expressed as cpm/μg of ependymal RNA. The relative rate of RNA synthesis is defined as the ratio of the CPM in RNA to the specific activity of the precursor pool per hour.

At intervals of 0, 4, 8, 12, 16, and 20 h after thyroxine treatment, other larvae were administered 1 μg/g body weight of actinomycin D (gift of Merck, Sharpe and Dohme, Rahway, N. J.). These tadpoles were sacrificed at 4-h intervals. 1 h before sacrifice, each animal received tritiated uridine, and the radioactivity in the nucleotide pool as well as in the PCA-precipitable RNA was measured as previously described.

Incorporation of [^3H]Leucine

The incorporation of L-[4,5-^{3}H]leucine (sp act 50 Ci/mmol, ICN Isotope and Nuclear Division, Irvine, Calif.) into trichloroacetic acid (TCA)-precipitable protein was determined at 0, 4, 8, 12, 16, 20, 24, 36, and 48 h after hormone treatment. 30 min before sacrifice, each tadpole received 1 μCi/g body weight of the isotope. The ependymae of five larvae were dissected into ice-cold 20% TCA, homogenized, and then centrifuged. Changes in the amino acid pool size were assessed by measuring the amount of radioactivity in the supernate of the TCA homogenate. The "20%" TCA residue was washed and heated in 5% TCA to release nucleic acids, and then lipids were extracted with acetone followed by a chloroform-methanol (2:1 vol/vol) mixture. The insoluble material was dissolved in hot 1 N NaOH, and one aliquot was mixed with scintillation fluid while another was used to measure ependymal protein (24).

1 h before the 12-, 16-, 20-, 24-, and 28-h intervals, 20 μg/g body weight of cycloheximide (Sigma Chemical Co.) were injected intraperitoneally. Tadpoles were sacrificed at 4-h periods during the succeeding 24 h, and 30 min before sacrifice each larva also received 1 μCi/g body weight of the isotope. Radioactivity was determined in the amino acid pool and the TCA-insoluble fraction as well.

OBSERVATIONS

Morphology of "Hypophysectomized" Ependymal Junctions

Two distinctive cell types are obvious in thin sections and freeze-fracture replicas of the "hypophysectomized" medullary ependyma (Figs. 1, 2). One is primarily ciliated (Fig. 1) while the other displays microvilli of varying dimensions (Fig. 2). At the lumen of the epithelium, microvilli of adjacent cells often fold over and interdigitate with one another. At such locales, microvillar membrane structure is frequently modified in some fashion, with desmosomes, fasciae adherentes, and even gap junctions perceptible alterations. In contrast, the junctional complex, which adjoins these cells at their apical surface, is comprised of a zonula adherens (Fig. 1). In freeze-fracture replicas (Fig. 2), this region of the plasma membrane discloses no distinguishing particle arrays or other unusual modifications (29). Occasionally, however, the uniformity of the adhering zonule is interrupted by a solitary gap junction (Fig. 1, *inset;* Fig. 2, *inset*) (6). The features of this pseudostratified epithelium are retained indefinitely unless the hypophysectomized tadpole receives thyroid hormone(s).

Influence of Thyroxine on Ependymal Junctions

An intraperitoneal injection of DL-thyroxine elicits profound biochemical and morphological changes within anuran larvae in as little as 24–48 h (11). Ependymal cells respond by elaborating numerous profiles of rough endoplasmic reticulum (32) and many small, dense-cored vesicles which resemble the catecholamine granules described by

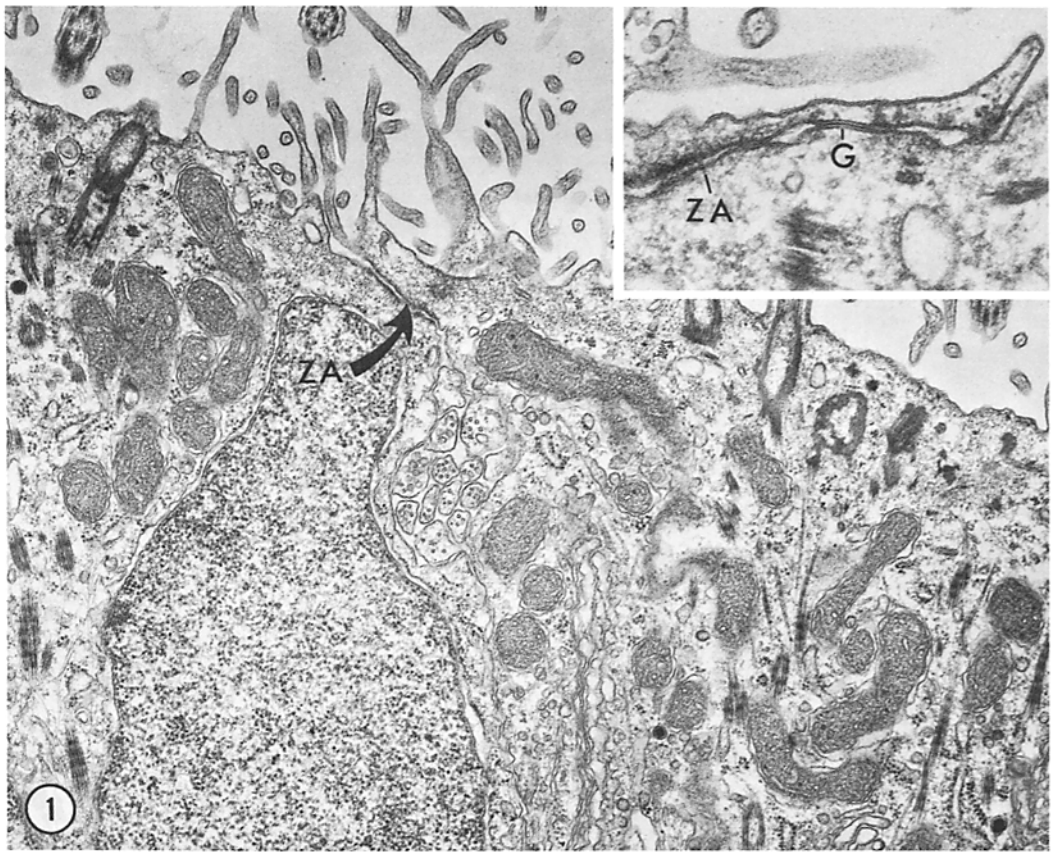

FIGURE 1 Morphology of "hypophysectomized" ependymal cells. Microvilli and cilia are prominent features of the luminal surface. Adjacent cells are joined to one another by a zonula adherens (*ZA*). The inset depicts a gap junction (*G*) which occasionally disrupts the continuity of the adhering zonule (*ZA*). × 15,000; *inset* × 65,000.

McKenna and Rosenbluth (27, 28) in subependymal cells of the toad hypothalamus. Alterations in the junctional configuration of these cells are most conspicuous 16–40 h after hormone administration. Thin sections reveal that the zonula adherens, which interconnects contiguous neuroepithelial cells, is subdivided by several gap junctions (Fig. 3). Further, thin sectioning unveils lengthy regions of close apposition between lateral plasmalemmas of adjacent cells (Fig. 4). Customarily, the width of this extracellular space ranges from 15 to 20 nm except at junctional sites (6); however, in these zones the dimensions of this space may vary from somewhat over 10 nm downward to 2 nm (Fig. 5). *En face* views of lanthanum-impregnated specimens further illustrate small groups of negatively stained profiles scattered throughout these regions (Fig. 7). Since many of these structures exhibit centrally stained spots and measure about 9–11 nm in diameter, they closely resemble the gap junction subunits observed by others (12, 29). Profiles of gap junctions are also prevalent in such areas (Figs. 4, 6).

Freeze-fracturing uncovers extensive regions of particle-free membrane on the A face of the plasma membrane 16–40 h after an injection of thyroxine. Gap junctions in all phases of construction can be discerned within the confines of these areas (Figs. 8–12). Loosely organized clusters, small aggregates, polarized arrays, and macular junctions are strikingly displayed in these immense "formation plaques" (18). The particles within the clusters and streams measure approximately 10 nm, whereas the granules within the aggregates and unmistakable gap junctions range between 8.5 and 9.0 nm in diameter (Fig. 10) (6). Although the plaques are not fully appreciated in B-face images, because of the normally sparse distribution of

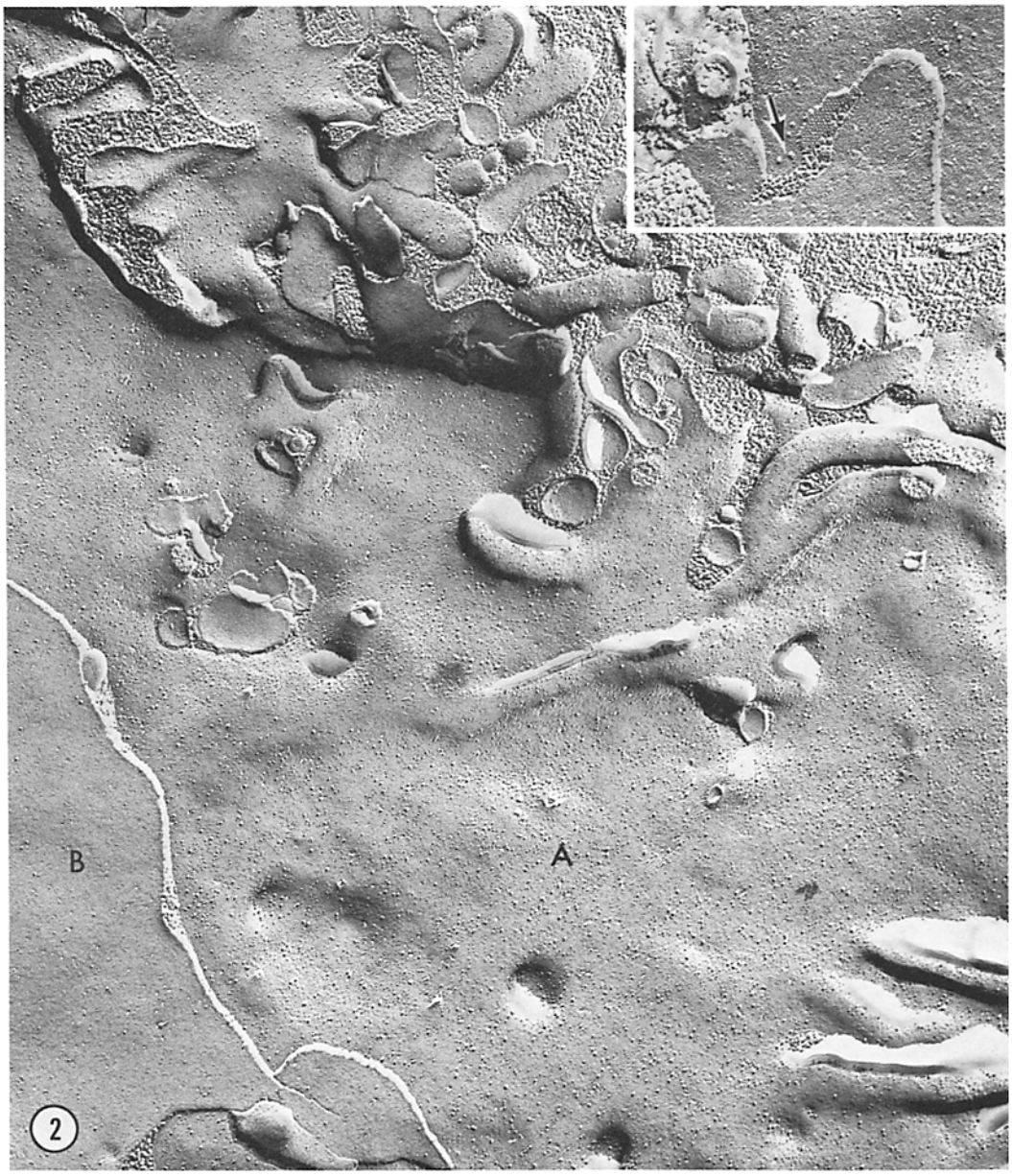

FIGURE 2 Freeze-cleaved appearance of the luminal surface of a "hypophysectomized" ependymal cell. Microvilli dominate the surface of this particular cell. The A face of the lateral plasma membrane displays numerous heterogeneous intramembrane particles distributed randomly, while the B face exhibits few particles. The inset illustrates a gap junction at the ependymal surface. Polygonally packed particles of the A face and pits of the B face are portrayed here. Note the 100-Å granules (arrow) nearby. × 40,000; *inset* × 50,000.

particles (29), all developmental stages are visible (Figs. 9, 11, 12).

A quantitative assessment of freeze-fracture replicas reveals that dramatic increases in formation plaque and gap junction area transpire between 16 and 40 h after hormone application (Figs. 13, 14). The area of A-face devoted to formation plaques rises from about 0.25 μm^2/100 μm^2 of A

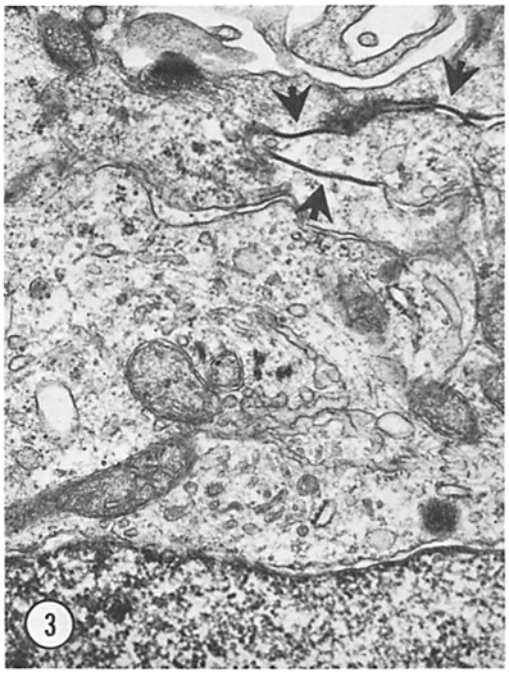

FIGURE 3 Junctional complex of an ependymal cell treated with thyroxine. K-pyroantimonate (1%) crisply stains gap junctions (arrowheads) which develop in the zonula adherens 36 h after hormone treatment. × 32,000.

face in controls to approximately 6.5 $\mu m^2/100\ \mu m^2$ of A-face after 40 h of hormone treatment (Fig. 13). This represents a 26-fold increase in formation plaque area on the A-face of the plasma membrane in response to hormone. Similarly, the area encompassed by gap junctions increases some 20-fold in this 24-h interim (Fig. 14). In absolute terms, 6.5% of the A face of the ependymoglial membrane surface becomes transformed into formation plaques, while only 1.25% of the membrane constitutes gap junctions. Hypophysectomized controls and normal stage VII larvae receiving a placebo exhibit no changes in either formation plaque or gap junction area during a similar period (Figs. 13, 14).

Thyroxine-Mediated Alterations in the Uptake and Incorporation of [^{3}H]Uridine and [^{3}H]Leucine

Thyroid hormones regulate many aspects of amphibian development (11). In particular, the hormone mediates the regression of some organs (21, 46) and the differentiation of others (5), ostensibly through a mechanism controlling the synthesis of RNA and protein. The present report demonstrates that the application of antibiotics which are known to impede RNA (actinomycin D) or protein (cycloheximide) synthesis interferes with the hormonally promoted glial differentiation and the formation of gap junctions.

One early response to thyroxine is a marked change in the levels of radioactivity present in the acid-soluble nucleotide pool. The uridine pool increases gradually during the first 8 h after hormone treatment and then exponentially in the succeeding 8 h (Fig. 15 A, Table I). At this juncture, acid-soluble radioactivity is fourfold higher than the controls (zero time values), whereas the incorporation of [^{3}H]uridine into PCA-insoluble material (RNA fraction) is elevated only marginally. However, between 16 and 24 h this pattern is reversed, with the uridine pool labeling declining precipitously as the incorporation of the isotope into the RNA fraction increases. During the latter half of the experimental period, there is little change in the specific activity of either the acid-soluble pool or the RNA fraction (Fig. 15 A, Table I). Although precursor measurements of this variety do not lend themselves to a direct determination of absolute synthetic rates, one may calculate a relative rate of synthesis (see Materials and Methods). Such a parameter reveals that there is a general decline in the rate of RNA synthesis during the first 16 h after the administration of thyroxine, followed by a dramatic rise in the succeeding 8 h (Fig. 15 B). These alterations in the relative rate of RNA synthesis accompany no overt changes in total RNA content as measured by the Schmidt-Thannhauser procedure (Fig. 15 B).

The incorporation of [^{3}H]uridine into the RNA fraction is inhibited 65–75% (Table I) if actinomycin D is administered simultaneously with thyroxine. This inhibitory action is restricted primarily to PCA-insoluble material since the specific activity of the acid-soluble pool remains essentially unchanged in response to the antibiotic (Table I). Similarly, introducing the drug at other intervals has much the same effect, i.e., inhibiting the labeling of RNA approximately 70%, while not influencing the specific activity of the pool (8).

Alterations in the leucine pool and the incorporation of [^{3}H]leucine into the ependymal protein are, likewise, dramatically altered by thyroxine (Fig. 16). During the first 20 h there is a sigmoidal increase in TCA-soluble pool labeling which is followed by a gradual decline in pool radioactivity

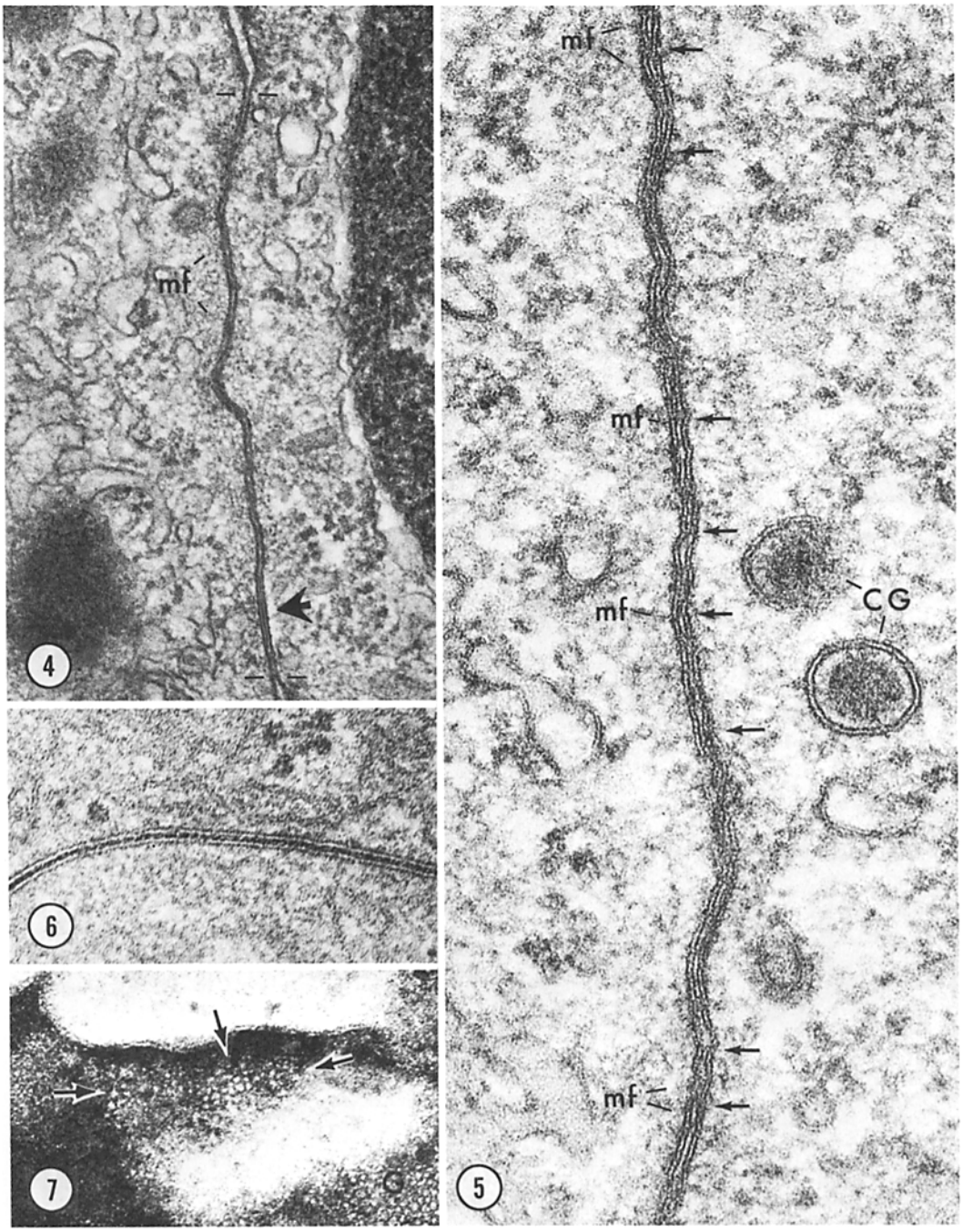

FIGURES 4 and 5 Thin sections of probable formation plaques induced by thyroxine. Fig. 4 discloses a long region of close membrane apposition (brackets) which is apparent 24 h after hormone treatment. Gap junctions (arrowhead) are frequently seen in such areas. A lacy network of microfilaments (*mf*) is also evident subjacent to the plaque membranes. Fig. 5 illustrates a small portion of another plaque 22 h after hormone treatment. There are many points (arrows) at which the extracellular space is reduced to ~20 Å; microfilaments (*mf*) may be attached to the outer leaflets at such sites along the plaque. CG, catecholamine-like granules. Fig. 4, × 45,000; Fig. 5, × 150,000.

FIGURES 6 and 7 Heavy metal tracers delineate the structure of the formation plaques. K-pyroantimonate (5%) fills the 20-Å extracellular space of a gap junction in a plaque area (Fig. 6). Face views of specimens treated with lanthanum demonstrate several small patches (arrows) which may represent gap precursor particles. Note the gap junction (*G*). Fig. 6, × 180,000; Fig. 7, × 150,000.

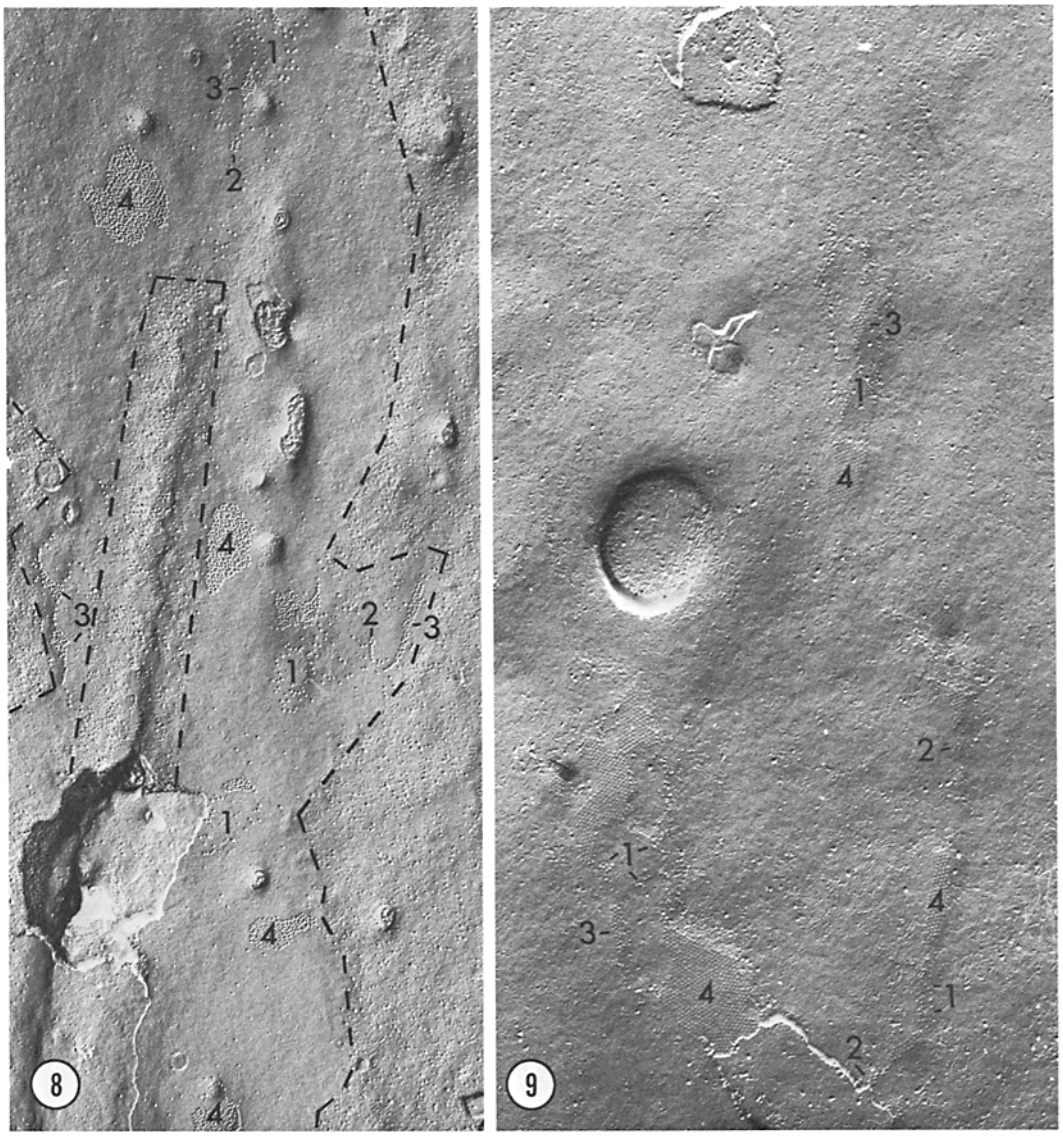

FIGURES 8 and 9 Freeze-fracture appearance of the A (Fig. 8) and B (Fig. 9) faces of formation plaques induced by thyroxine. At 28 (Fig. 8) or 30 (Fig. 9) h particle clusters (*1*), aggregates (*2*), "growing" junctions (*3*), and "macular" junctions (*4*) are visible within the smooth regions of the plaques. The author conceives of gap junctions passing through the four developmental stages with the cluster representing the earliest phase and the macular junction the most mature stage. Formation plaque area is confined within the limits of the dashed line. Fig. 8, × 40,000; Fig. 9, × 60,000

during the subsequent 1.5 days. The incorporation of [^{3}H]leucine into the TCA-insoluble residue diminishes rather slowly for 16 h and then increases linearly through the remainder of the experimental period (Fig. 16 A). The relative rate of protein synthesis falls to about 25% of control levels (zero time value) during the first 16 h of hormone treatment; then it increases significantly as exposure to the hormone continues (Fig. 16 B). A sustained decline in total ependymal protein accompanies the changes noted in the leucine labeling of the amino acid pool and TCA-insoluble material (Fig. 16 A, B).

The injection of cycloheximide at several intervals after hormone treatment inhibits the incorporation of [^{3}H]leucine into TCA-insoluble material

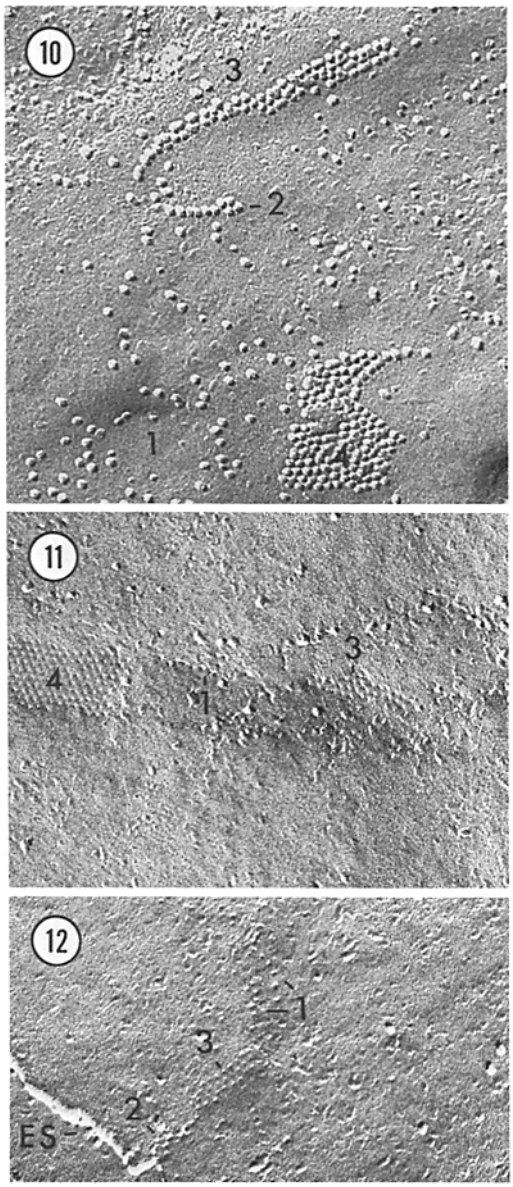

FIGURES 10–12 A- and B-face profiles of developing gap junctions induced by thyroxine. Fig. 10 depicts several aspects of junctional assembly, including clustering (*1*), aggregation (*2*), "growing" (*3*), and "macular" (*4*) junctions. Figs. 11 and 12 illustrate several developmental stages in B-face images. *ES*, extracellular space. Figs. 10–12, × 112,500.

80–90% (Fig. 17 B), while not significantly altering the labeling patterns of the leucine pool (Fig. 17 A). Only with prolonged exposure (>20 h) is the specific activity in the acid-soluble pool affected (Fig. 17 A) by the drug.

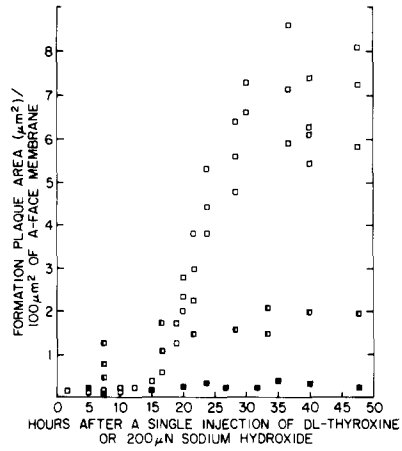

FIGURE 13 Alterations in formation plaque area as a function of time after a single injection of DL-thyroxine (T_4) or NaOH. Hypophysectomized larvae (□) were administered T_4 at time zero, whereas other hypophysectomized larvae (■) and normal stage VII controls (◧) received NaOH. Each square represents the average area of 10 plaques derived from one animal.

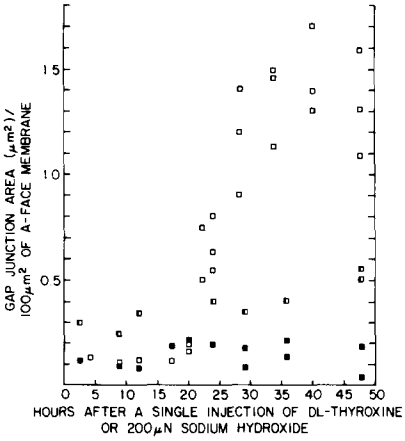

FIGURE 14 Changes in gap junction area as a function of time after a single injection of DL-thyroxine (T_4) or NaOH. Hypophysectomized larvae (□) were treated with T_4 at time zero, while other hypophysectomized larvae (■) and normal stage VII controls (◧) received NaOH at the same time. Each symbol represents the data acquired from one animal.

Effects of Actinomycin D and Cycloheximide on Developing Gap Junctions

Though actinomycin D substantially inhibits the incorporation of [^{3}H]uridine into RNA throughout development, it affects the formation of gap junctions only during the first 12 h after hormone treatment. Under these circumstances, thin sec-

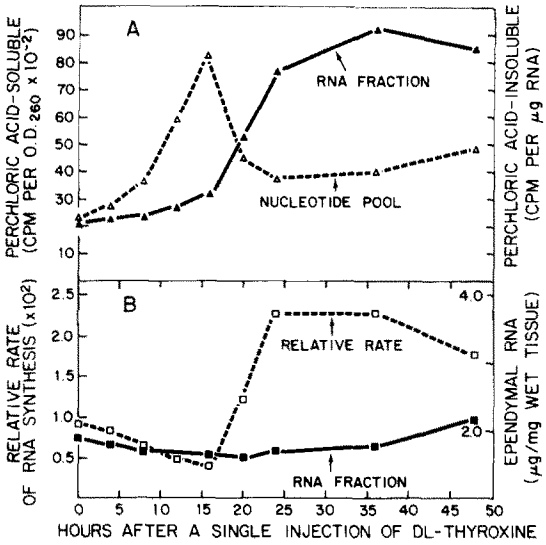

FIGURE 15 A Uptake of [³H]uridine into PCA-soluble (nucleotide pool) and PCA-insoluble (RNA) fractions of ependyma after treatment with DL-thyroxine. Each symbol is the average value of three experiments. B, Influence of DL-thyroxine on the relative rate of RNA synthesis. The rate (□) was derived from the data in Fig. 15 A (see Materials and Methods). Total RNA (■) measured by the Schmidt-Thannhauser procedure is also plotted. Each point is the average of three determinations.

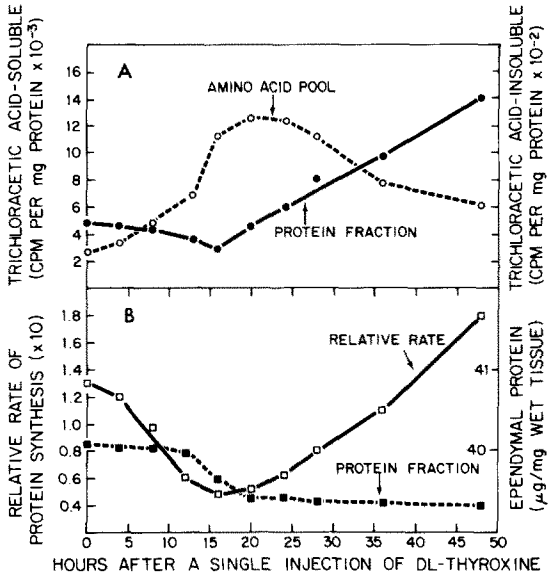

FIGURE 16 A Uptake and incorporation of [³H]leucine in TCA-soluble (amino acid pool) and TCA-insoluble (protein) fractions of ependyma after treatment with DL-thyroxine. Each point represents the average value of four experiments. B, The relative rate of protein synthesis (□) and protein content (■) of ependyma after a single injection of DL-thyroxine. Protein was assayed by the Lowry procedure. Each symbol is an average value of four experiments.

TABLE I

Effects of Actinomycin D (AMD) on the Uptake and Incorporation of [³H]Uridine‡*

Time of sacrifice	Number of experiments	AMD	Acid-soluble pool	Specific activity of RNA	Inhibition of [³H]Uridine uptake into RNA
h		*1 μg/g body wt*	*cpm/OD₂₆₀§*	*cpm/μg RNA§*	
0	3	–	2,440	21	0
	4	+	2,355	7	70%
4	4	–	2,675	22	0
	4	+	2,720	7	69%
8	3	–	3,630	23	0
	5	+	3,340	8	67%
12	3	–	5,800	26	0
	4	+	5,410	7	72%
16	4	–	8,260	32	0
	4	+	7,940	10	68%
24	3	–	3,760	77	0
	3	+	3,550	27	65%
36	3	–	3,970	92	0
	3	+	3,840	24	74%

* All larvae received 1 μg/g body wt of DL-thyroxine at time 0 as well as 1 μg/g body wt of AMD (+) or 200 μN NaOH (–) at specified intervals.

‡ 1 h before sacrifice each larva was injected with 5 μCi/g body wt of [³H]uridine.

§ All values are averaged.

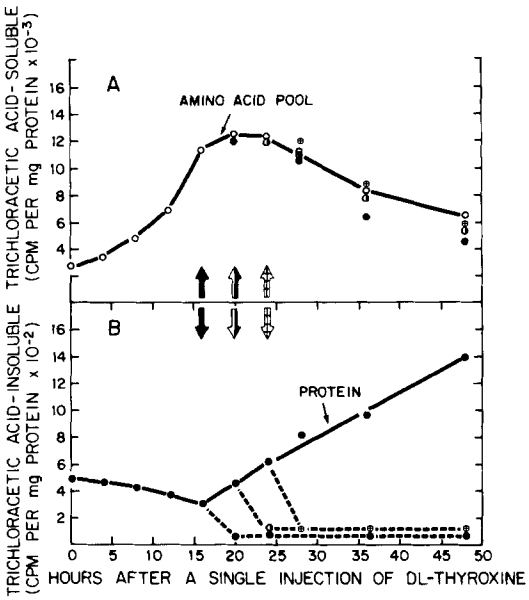

FIGURE 17 A Influence of cycloheximide (CHX) on the uptake of [^{3}H]leucine into the TCA-soluble pool after administration of DL-thyroxine. CHX was injected at 16 (▲), 20 (▲), or 24 (▲) h and the amino acid pool activity was determined at specified intervals (● ○ ⊕). Each point represents the average of four experiments. B, Effect of cycloheximide (CHX) on the incorporation of [^{3}H]leucine into TCA-insoluble fraction (protein) after hormone treatment. The schedule of drug injection was identical to that for Fig. 17 A. Each value is an average of four experiments.

tioning and freeze-cleaving disclose an undifferentiated ependyma with only a few randomly dispersed gap junctions. At a time when formation plaques normally appear in response to thyroxine (16–20 h), none are obvious if the larvae are treated with actinomycin D within 12 h of hormone application. However, injection of the antibiotic at 16 or 18 h after exposure to thyroxine does not markedly influence ependymoglial differentiation (appearance of rough endoplasmic reticulum and dense-cored granules) or the biogenesis of gap junctions. Particle clusters, aggregates, and macular junctions are prominent in freeze-fracture replicas (Fig. 18).

In contrast, cycloheximide has immediate and unequivocal effects on the formation of gap junctions. At doses (20 μg/g body weight) high enough to inhibit the incorporation of leucine into TCA-insoluble material by 90% (Fig. 17 B), cycloheximide halts junctional development at two stages. Arresting protein synthesis before 16 h completely prevents the genesis of formation plaques and gap junctions (Figs. 19, 20). Employing cycloheximide at 20 h, however, suppresses only the formation of developing junctions and not the appearance of formation plaques (Figs. 19, 20). Freeze-fracturing discloses novel alterations in the A face of the plasma membrane. Normally, the A face exhibits a random distribution of heterogeneous particles; but the treatment of larvae at this juncture with cycloheximide transforms the A face into regions which disclose few particles and others which exhibit high particle packing densities (compare Fig. 2 with Fig. 21). Although some of the particles in these smooth areas measure 100 Å, the only evidence of assembling junctions is a rare stream of large particles separating the two regions (Fig. 21). Except for the absence of clusters, aggregates, and differentiating junctions, these expanses of smooth membrane resemble the formation plaques induced by thyroxine. As cycloheximide is utilized at later intervals, various stages in the development

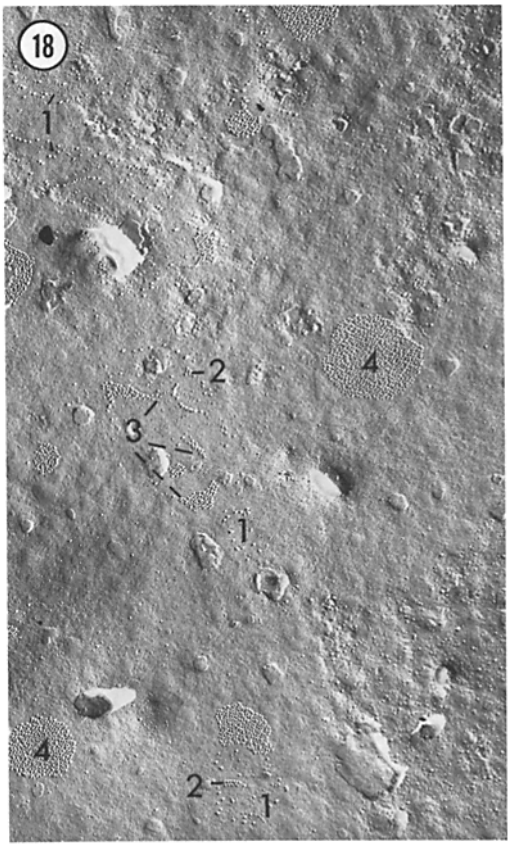

FIGURE 18 A-face replica of a 30-h old formation plaque induced by thryoxine followed 16 h later by actinomycin D treatment. Developmental stages seen here are identical to those in Fig. 8. × 43,000.

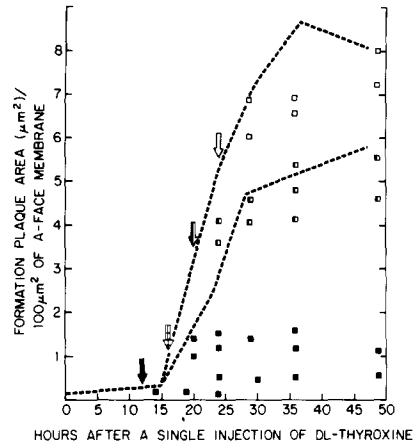

FIGURE 19 Influence of cycloheximide (CHX) on formation plaque area after the administration of DL-thyroxine. CHX was injected at 12 (▲), 16 (▲), 20 (▲), or 24 (△) h and larvae were sacrificed at specified intervals (■ ⊞ ◧ □). The area enclosed by the dashed line is the change in formation plaque area induced by thyroxine in the absence of CHX. Each point represents the data obtained from a single animal.

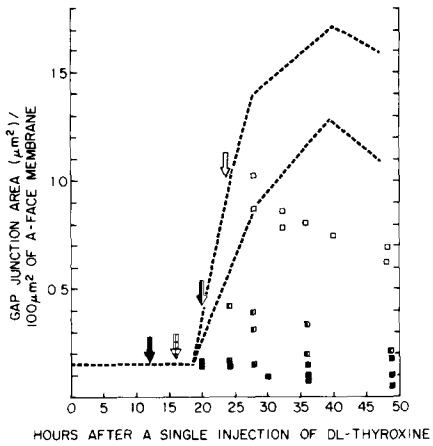

FIGURE 20 Effect of cycloheximide (CHX) on gap junction area after treatment with DL-thyroxine. CHX was administered at 12 (▲), 16 (▲), 20 (▲), or 24 (△) h and larvae were sacrificed at specified intervals (■ ⊞ ◧ □). The area outlined by the dashes represents the change in gap junction area induced by thyroxine in the absence of CHX. Each point is the data derived from one animal.

of the junctions can be recognized. Between 22 and 24 h, clusters (Fig. 22) and small aggregates may be readily appreciated in freeze-fracture replicas. When administration of the drug is delayed beyond 24 h, small variegated gap junctions are frequently observed within plaque regions (Fig. 23).

DISCUSSION

The development of the amphibian neuroepithelium can be subdivided into two distinct periods, one of which requires thyroid hormone for its initiation. In the first, neurons are apparently generated in the ventricular zone and subsequently migrate peripherally into intermediate grey matter. The second period, which is dependent on the presence of thyroid hormone, mediates ependymoglial differentiation (32). One facet of the ependymoglial response involves the development of gap junctions between contiguous neuroglial cells. Moreover, the propagation of these junctions seems to require the synthesis of new protein which may be predicated on an earlier period of RNA synthesis.

Gap Junction Differentiation

This study as well as others (3, 18) confirms our previous impressions (6) that the formation of gap junctions proceeds in discrete steps. As early as 16–20 h after a single injection of DL-thyroxine, large formation plaques (18) appear between adjacent ependymoglial cells. Within the limits of these plaques, all aspects of gap junction assembly are perceptible (Figs. 8, 10). Large clusters of 10-nm particles previously described in reaggregating Novikoff hepatoma cells (18) are confirmed in this report. Small particle aggregates as well as diminutive arrays displaying a variety of contours are also prominent (Fig. 8) and probably represent stages in the formation of gap junctions (6, 18, 36). Similarly, thin sections reveal unusual expanses of cell-cell contact in which the extracellular space is reduced to 10 nm or less (Figs. 4, 5). It is these areas, in all likelihood, which denote the formation plaques described here and those reported by Johnson et al. (18). A preliminary report from Johnson's laboratory (17) further discloses that the invertebrate hormone, ecdysterone, apparently alters the particle packing density and morphology of *Limulus* gap junctions (19). Here, loosely packed arrays recognized from 1 to 3 days after hormonal administration are interpreted as reflecting a phase of gap junction development.

The origin of the 10-nm gap precursor particles is still a moot issue. These large particles which are so characteristic of differentiating junctions are rarely encountered in freeze-fracture replicas of mature tissues (12, 29). However, subjecting rat liver hepatocytes to hypertonic shock has demon-

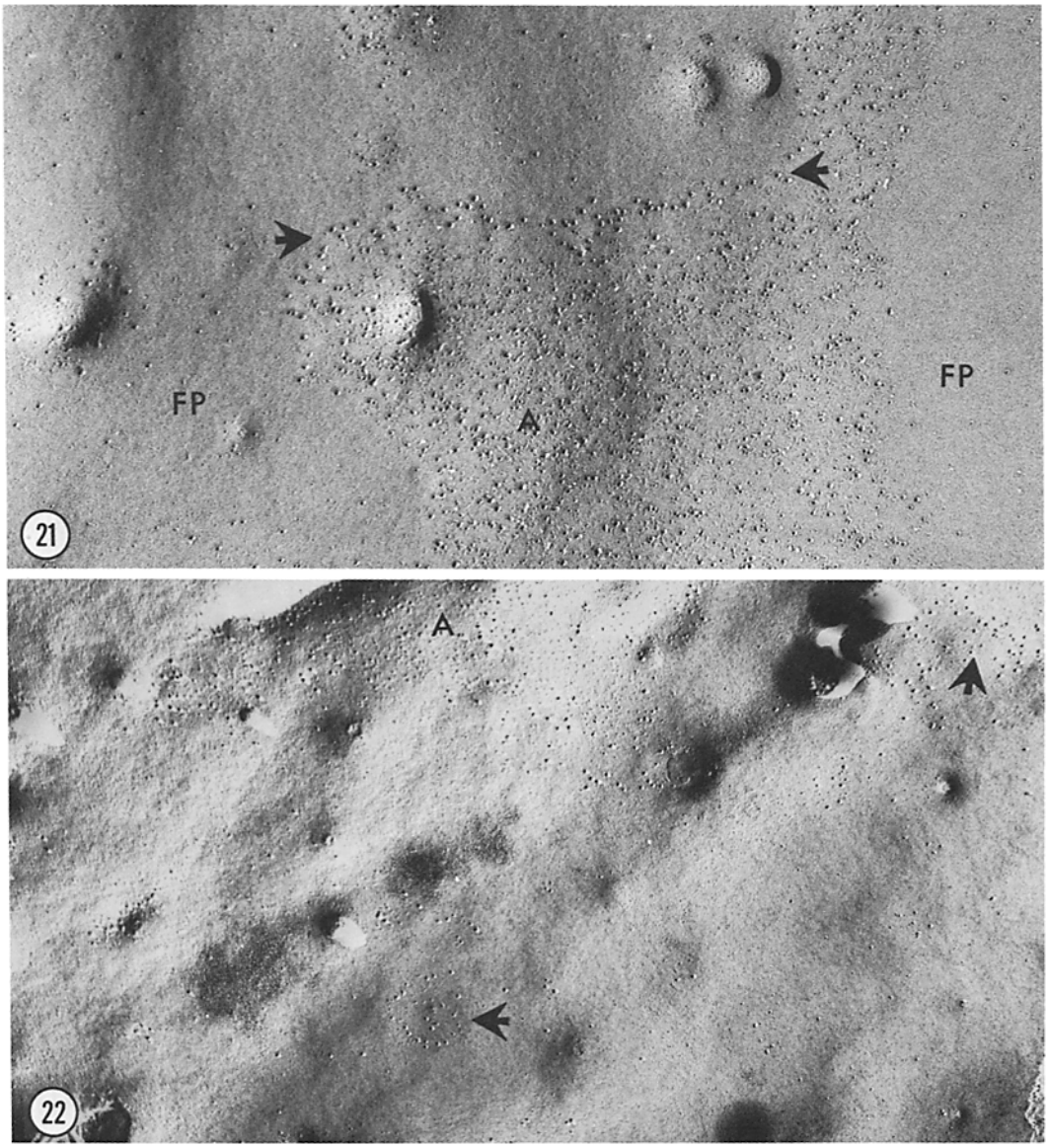

FIGURE 21 A-face replica of the transition zone between a formation plaque (*FP*) induced by thyroxine followed by cycloheximide treatment at 20 h with fixation at 26 h. Note the sharp distinction between "normal" A face and the plaque region and the large particles dispersed somewhat haphazardly in the plaque (*FP*). At the boundary between the A face and the plaque, a row of 100-Å granules (arrowheads) is visible. × 50,000.

FIGURE 22 A-face profile of a formation plaque (*FP*) in which larva received cycloheximide at 22 h and was fixed at 28 h after hormone. Two clusters of 100-Å granules can be discerned (arrowheads) in this large formation plaque. The "normal" A face is also pictured. × 45,000.

strated the existence of a similar class of particles residing around the periphery of gap junctions (15). Perhaps, as the junction is disrupted, the conformation of its outer particles is altered, revealing their larger dimension. Similarly, in the assembly of the junction, changes in particle size may accompany the polygonal packing of subunits into recognizable junctions (6, 18).

FIGURE 23 Another A-face image of a formation plaque in which the larva received cycloheximide at 28 h and was fixed at 38 h after hormone. Particle arrays and two gap junctions (*G*) are apparent in the formation plaque. Note the A face nearby. × 50,000.

Macromolecular Synthesis during Gap Junction Assembly

Although gap junctions may develop independently of protein synthesis in reaggregating Novikoff hepatoma cells (9, 40), there appears to be an obligatory requirement of new protein synthesis for the assembly of junctions during thyroxine-stimulated ependymoglial differentiation. Cycloheximide as well as actinomycin D markedly influences junctional development if administered at the proper time after hormone treatment.

Inhibiting protein synthesis with cycloheximide (Fig. 17 B) at various intervals after the injection of thyroxine may directly affect the development of formation plaques and the production of gap-junction subunits. Formation plaques as well as gap junctions fail to appear if cycloheximide is employed at 16 h after hormone treatment. Freeze-cleaving reveals an A face which exhibits a heterogeneous class of randomly dispersed particles. Likewise, thin sections fail to illustrate the elaborate regions of close cell-cell contact that are common at this juncture. At 20 h some formation plaques are evident (Fig. 21), but gap precursors are not yet visible and there appears to be no thin-section correlate of these plaques. The boundary between the plaque and "normal" A-face membranes is sharp and well defined, rarely displaying a linear arrangement of 10-nm granules (Fig. 21). Between 22 and 24 h, clusters (Fig. 22) and small aggregates appear; however, if cycloheximide treatment is delayed to 24 h or later, then the formation plaques reveal clusters, aggregates, and recognizable gap junctions (Fig. 23). This sequential inhibition of plaque formation and junctional assembly suggests that the production of new protein(s) is a prerequisite for both development of the plaques and the differentiation of junctions.

Alternatively, it is also conceivable that cycloheximide may primarily interfere with cell-cell interactions and only secondarily with the production of gap junctions; thus, the suppression of cell-cell recognition and subsequent contact may obstruct the development of gap junctions between differentiating glia. The inhibition of myoblast contact in vitro with cycloheximide (47) could prevent the genesis of gap junctions and the establishment of low-resistance coupling (33, 34) in such a fashion. In other instances, the inhibition of protein synthesis is known to impede histotypic cell reaggregation of trypsinized chick embryo brain cells (22, 25, 30, 31). It is probable that this cycloheximide-sensitive step may involve the renewal of an aggregating factor on the cell surface which is altered through the proteolytic action of trypsin (2, 22, 26). However, it must be emphasized that the inhibition of protein synthesis during the first 1 or 2 h of reaggregation has little noticeable influence on the appearance of gap junctions (41). Ethylenediamine tetraacetate (EDTA), which is also commonly employed to dissociate embryonic and cultured cells, has minimal effects on the early phases of cell aggregation (18, 25). In such experiments, cell-cell interactions and gap junction formation occur for at least 2 h in the absence of protein synthesis (9). If gap junction particles represent integral membrane proteins (13, 14, 16, 44), then it is unlikely that the dissociation of Novikoff hepatoma cells in EDTA, for example, would result in their removal from

the plasma membrane (43, 39). Thus, the chelation of extracellular cations, such as calcium (23, 37), or the alteration of some other factor may affect the distribution of gap particles possibly by disrupting their extracellular channels (4). Resuspending such cells in aggregation medium would resupply this vital constituent and initiate junctional formation in the absence of protein synthesis (9, 40).

Direct comparisons of junctional assembly between reaggregating cell systems and differentiating glia must be interpreted with caution. Since gap junctions are known to join embryonic (4, 7) and Novikoff hepatoma (20) cells before dissociation, perhaps a limited pool of gap precursors and aggregating factors reside in the plasma membranes of the separated cells, so that cell reaggregation and gap-junction development may be sustained for at least 2 h in the absence of protein synthesis. Conversely, ependymoglial cells first appear in response to thyroid hormone (28). Consequently, glial differentiation would, out of neccessity, require membrane differentiation which could include the elaboration of glial-glial recognition factors and gap junctions. Under the present circumstances, it is not possible to discern whether the inhibition of protein synthesis with cycloheximide is initially affecting cell-cell recognition, junctional formation, or both.

Actinomycin D only affects junctional assembly during the first 12 h after hormone treatment. Although this antibiotic only inhibits the incorporation of [^{3}H]uridine into acid-precipitable RNA approximately 70%, it fully prevents the development of formation plaques and gap junctions. Nevertheless, if application of the drug is delayed beyond 12 h, ependymoglial cells apparently differentiate normally with formation plaques exhibiting features that are indistinguishable from thyroxine-treated controls (Fig. 18). Even though no attempt was made to characterize new ependymal RNAs, the observations of Ryffel and Weber (38, 39) indicate that thyroxine enhances the synthesis of tadpole brain ribosomal and transfer RNA, but apparently does not induce the production of RNAs with messenger qualities. Whether gap proteins or any other proteins associated with junctional formation are translanted from newly constructed cytoplasmic ribosomes or rough endoplasmic reticulum (32) requires further investigation; however, the effects of actinomycin D allude to the need for a template.

This investigation concludes that the assembly of gap junctions between differentiating ependymoglial cells is enhanced by thyroxine. The hormone-mediated development of these junctions requires the synthesis of new protein which appears essential to the genesis of formation plaques as well as the production of gap junction subunits. The temporal appearance of formation plaques followed by their population with gap junction precursors and developing junctions suggests that gap subunits are synthesized de novo and then inserted in some fashion into the formation plaque membrane.

The author wishes to express his most sincere thanks to Ms. Paulette Saddler and Ms. Mary Owens for typing the manuscript.

This study was supported by a National Institutes of Health Grant, GM21698, and by a University of Texas Institutional Grant, N14135, awarded to the author.

Received for publication 1 May 1975, and in revised form 4 February 1976.

REFERENCES

1. ALBERTINI, D. F., and E. ANDERSON. 1975. Structural modifications of lutein cell gap junctions during pregnancy in the rat and the mouse. *Anat. Rec.* **181**:171–194.
2. BALSAMO, J., and J. R. LILIEN. 1974. Embryonic cell aggregation: kinetics and specificity of binding of enhancing factors. *Proc. Natl. Acad. Sci. U. S. A.* **71**:727–731.
3. BENEDETTI, E. L., I. DUNIA, and H. BLOEMENDAL. 1974. Development of junctions during differentiation of lens fibers. *Proc. Natl. Acad. Sci. U. S. A.* **71**:5073–5077.
4. BENNETT, M. V. L. 1973. Function of electrotonic junctions in embryonic and adult tissue. *Fed. Proc.* **32**:65–75.
5. COHEN, P. P. 1970. Biochemical differentiation during amphibian metamorphosis. *Science (Wash. D.C.).* **168**:533–543.
6. DECKER, R. S., and D. S. FRIEND. 1974. Assembly of gap junctions during amphibian neurulation. *J. Cell Biol.* **62**:32–47.
7. DEHAAN, R. L., and H. G. SACHS. 1972. Cell coupling in developing systems: the heart-cell paradigm. *Curr. Top. Dev. Biol.* **7**:193–228.
8. EATON, J. E., JR., and E. FRIEDEN. 1969. Primary mechanisms of thyroid hormone control of amphibian metamorphosis. *Gen. Comp. Endocrinol. Suppl.* **2**:398–407.
9. EPSTEIN, M., and J. SHERIDAN. 1974. Formation of low-resistance junctions in the absence of protein synthesis and metabolic energy production. *J. Cell Biol.* **63**(2, Pt. 2):95 a. (Abstr.).

10. FLECK, A., and H. N. MUNRO. 1962. The precision of ultraviolet absorption measurements in the Schmidt-Thannhauser procedure for nucleic acid estimation. *Biochem. Biophys. Acta.* **55**:571–583.
11. FRIEDEN, E., and J. J. JUST. 1970. Hormonal responses in amphibian metamorphosis. *In* Biochemical Actions of Hormones. G. Litwack, editor. Academic Press, Inc., New York. 1–52.
12. GILULA, N. B. 1974. Isolation of rat liver gap junctions and characterization of the polypeptides. *J. Cell Biol.* **63**(2, Pt. 2):111 a. (Abstr.).
13. GILULA, N. B. 1974. Junctions between cells. *In* Cell Communication. R. P. Cox, editor. John Wiley & Sons, New York. 1–29.
14. GOODENOUGH, D. A. 1974. Bulk isolation of mouse hepatocyte gap junction. Characterization of the principal protein, connexin. *J. Cell Biol.* **61**:557–563.
15. GOODENOUGH, D. A., and N. B. GILULA. 1974. The splitting of hepatocyte gap junctions and zonulae occludentes with hypertonic disaccharides. *J. Cell Biol* **61**:575–590.
16. GOODENOUGH, D. A., and W. STOCKENIUS. 1972. The isolation of mouse hepatocyte gap junctions. Preliminary chemical characterization and X-ray diffraction. *J. Cell Biol.* **54**:646–656.
17. JOHNSON, G., D. QUICK, R. JOHNSON, and W. HERMAN. 1974. Influence of hormones on gap junctions in horseshoe crabs. *J. Cell Biol.* **63**(2, Pt. 2):157 a. (Abstr.).
18. JOHNSON, R. G., M. HAMMER, J. SHERIDAN, and J. P. REVEL. 1974. Gap junction formation between reaggregated Novikoff Hepatoma cells. *Proc. Natl. Acad. Sci. U. S. A.* **71**:4536–4540.
19. JOHNSON, R. G., W. S. HERMAN, and D. M. PREUS. 1973. Homocellular and heterocellular gap junctions in *Limulus*: a thin section and freeze-fracture study. *J. Ultrastruct. Res.* **43**:298–312.
20. JOHNSON, R. G., and J. D. SHERIDAN. 1971. Junctions between cancer cells in culture: ultrastructure and permeability. *Science (Wash. D.C.).* **174**:717–719.
21. KIM, K. H., and K. A. SLICKERS. 1971. Biochemistry of anuran pancreas development during thyroxine-induced metamorphosis. *In* Hormones in Development. M. Hamburgh and E. J. W. Barrington, editors. Appleton, Century, Crofts, New York. 321–334.
22. LILIEN, J. 1968. Specific enhancement of cell aggregation *in vitro*. *Dev. Biol.* **17**:657–678.
23. LOEWENSTEIN, W. R. 1967. Cell surface membranes in close contact. Role of calcium and magnesium ions. *J. Colloid. Interface Sci.* **25**:34–46.
24. LOWRY, O. H., N. J. ROSEBROUGH, A. L. FARR, and R. J. RANDALL. 1951. Protein measurement with the Folin-phenol reagent. *J. Biol. Chem.* **193**:265–275.
25. MCCLAY, D. R., and S. R. BAKER. 1975. A kinetic study of embryonic cell adhesion. *Dev. Biol.* **43**:109–122.
26. MCCLAY, D. R., and A. A. MOSCONA. 1974. Purification of specific cell aggregating factor from embryonic neural retinal cells. *Exp. Cell Res.* **87**:438–443.
27. MCKENNA, O., and J. ROSENBLUTH. 1971. Characterization of an unusual catecholamine-containing cell type in the toad hypothalamus. A correlated ultrastructural and fluorescence histochemical study. *J. Cell Biol.* **48**:650–672.
28. MCKENNA, O., and J. ROSENBLUTH. 1975. Ontogenetic studies of a catecholamine-containing nucleus of the toad hypothalamus in relation to metamorphosis. *Exp. Neurol.* **46**:495–505.
29. MCNUTT, N. S., and R. S. WEINSTEIN. 1973. Membrane ultrastructural at mammalian intercellular junctions. *Prog. Biophys. Mol. Biol.* **26**:45–107.
30. MOSCONA, M. H., and A. A. MOSCONA. 1963. Inhibition of adhesiveness and aggregation of dissociated cells by inhibitors of protein and RNA synthesis. *Science (Wash. D.C.).* **142**:1070–1072.
31. MOSCONA, M. H., and A. A. MOSCONA. 1966. Inhibition of cell aggregation *in vitro* by puromycin. *Exp. Cell Res.* **41**:703–706.
32. PESETSKY, I., and P. G. MODEL. 1971. Thyroxine-dependent glial activation in the developing central nervous system of amphibians. *In* Hormones in Development. M. Hamburgh and E. J. W. Barrington, editors. Appleton, Century, Crofts, New York. 335–344.
33. RASH, J. E., and D. FAMBROUGH. 1973. Ultrastructural and electrophysiological correlates of cell coupling and cytoplasmic fusion during myogenesis *in vitro*. *Dev. Biol.* **30**:166–186.
34. RASH, J. E., and L. STAEHELIN. 1974. Freeze-cleave demonstration of gap junctions between skeletal cells *in vivo*. *Dev. Biol.* **36**:455–461.
35. REVEL, J. P. 1974. Some aspects of cellular interactions in development. *In* The Cell Surface in Development. A. A. Moscona, editor. John Wiley & Son, New York. 51–66.
36. REVEL, J. P., L. CHANG, and P. YIP. 1973. Cell junctions in the early chick embryo: a freeze-etch study. *Dev. Biol.* **35**:302–317.
37. ROSE, B., and W. R. LOEWENSTEIN. 1971. Junctional membrane permeability. Depression by substitution of Li for extracellular Na, and by long term lack of Ca and Mg; restoration of cell repolarization. *J. Membr. Biol.* **5**:20–50.
38. RYFFEL, G., and R. WEBER. 1971. Kennzeichnunzder RNS aus verschiedenen Organen von Xenopuslarven und ihre Beeinflussung durch Thyroxin. *Rev. Suisse Zool.* **78**:639–650.
39. RYFFEL, G., and R. WEBER. 1973. Changes in the pattern of RNA synthesis in different tissues of *Xenopus* larvae during induced metamorphosis. *Exp. Cell Res.* **77**:79–88.
40. SHERIDAN, J. D. 1974. Low-resistance junctions: some functional considerations. *In* The Cell Surface

in Development. A. A. Moscona, editor. John Wiley & Sons, New York. 187–206.
41. SHIMADA, Y., A. A. MOSCONA, and D. A. FISCHMAN. 1974. Scanning electron microscopy of cell aggregation: cardiac and mixed retina-cardiac cell suspensions. *Dev. Biol.* **36**:428–446.
42. SHUMWAY, W. 1940. Stages in the normal development of *Rana pipiens*. I. External form. *Anat. Rec.* **78**:139–144.
43. SINGER, S. J. 1974. The molecular organization of membranes. *Annu. Rev. Biochem.* **43**:805–833.
44. SINGER, S. J., and G. L. NICOLSON. 1972. The fluid mosaic model of the structure of cell membranes. *Science* (*Wash. D.C.*). **175**:720–731.
45. TAYLOR, C. A., and J. J. KOLLROS. 1946. Stages in the normal development, *Rana pipiens* larvae. *Anat. Rec.* **94**: 7–24.
46. Weber, R. 1969. The isolated tadpole tail as a model system for studies on the mechanism of hormone-dependent tissue involution. *Gen. Comp. Endocrinol. Suppl.* **2**:408–416.
47. YAFFE, D., and H. DYM. 1973. Gene expression during differentiation of contractile muscle fibers. *Cold Spring Harbor Symp. Quant. Biol.* **37**:543–546.
48. YEE, A. G. 1972. Gap junctions between hepatocytes in regenerating liver. *J. Cell Biol.* **55**(2, Pt. 2):294 a. (Abstr.).
49. ZAMPIGHI, G., and J. D. ROBERTSON. 1973. Fine structure of the synaptic discs separated from goldfish medulla oblongata. *J. Cell Biol.* **56**:92–105.